Rapid changes of glacial climate simulated in a coupled climate model

Andrey Ganopolski & Stefan Rahmstorf

Potsdam Institute for Climate Impact Research, PO Box 60 12 03, 14412 Potsdam, Germany

Abrupt changes in climate, termed Dansgaard–Oeschger and Heinrich events, have punctuated the last glacial period (~100–10 kyr ago) but not the Holocene (the past 10 kyr). Here we use an intermediate-complexity climate model to investigate the stability of glacial climate, and we find that only one mode of Atlantic Ocean circulation is stable: a cold mode with deep water formation in the Atlantic Ocean south of Iceland. However, a 'warm' circulation mode similar to the present-day Atlantic Ocean is only marginally unstable, and temporary transitions to this warm mode can easily be triggered. This leads to abrupt warm events in the model which share many characteristics of the observed Dansgaard–Oeschger events. For a large freshwater input (such as a large release of icebergs), the model's deep water formation is temporarily switched off, causing no strong cooling in Greenland but warming in Antarctica, as is observed for Heinrich events. Our stability analysis provides an explanation why glacial climate is much more variable than Holocene climate.

Two main types of abrupt climate changes have punctuated the last glacial period: Dansgaard–Oeschger (D/O) events and Heinrich events[1–8]. D/O events typically start with an abrupt warming of Greenland by 5–10 °C over a few decades or less, followed by gradual cooling over several hundred or several thousand years. This cooling phase often ends with an abrupt final reduction of temperature back to cold ('stadial') conditions. D/O climate change is centred on the North Atlantic and on regions with strong atmospheric response to changes in that area, and shows only a weak response in the Southern Ocean or Antarctica. The 'waiting time' between successive D/O events is most often around 1,500 years, or, with decreasing probability, near 3,000 or 4,500 years (ref. 9). This suggests the existence of an as-yet unexplained 1,500-year cycle which often (but not always) triggers a D/O event.

Heinrich events[1,5] involve surging of the Laurentide Ice Sheet that covered northern America at the time, and occur in the cold, stadial phase of some D/O cycles. They have a variable spacing of several thousand years. Sediment data suggest that Heinrich events shut down, or at least drastically reduce, the formation of North Atlantic Deep Water (NADW). Records from the South Atlantic Ocean and parts of Antarctica show that the cold Heinrich events in the North Atlantic were associated with unusual warming there (the 'bipolar see-saw effect'[10–12]). Sediment data also suggest that changes in the Atlantic thermohaline circulation are crucial in these abrupt climate changes[13,14], and it is difficult to imagine a mechanism for such dramatic and rapid temperature changes that does not involve large changes in ocean heat transport.

Many modelling studies in the past have shown that the Atlantic thermohaline circulation (1) is a significant contributor to the regional heat budget over the North Atlantic region, (2) is sensitive to freshwater input into the North Atlantic, and (3) is a nonlinear system with thresholds for transitions between qualitatively different circulation modes. However, previous attempts to simulate the general sensitivity to freshwater input or more specific climate events of the glacial period have been based on perturbations to the modern, rather than to a glacial, modelled climate state. This approach has the obvious limitation that the stability properties of the glacial climate could have been very different from those of the present climate.

Here we present a stability analysis of glacial climate and simulations of D/O and Heinrich events, based on the glacial background climate as simulated in ref. 15. We show that the stability properties of glacial climate differ fundamentally from those of the present climate in our model, and that taking this into account resolves a number of the paradoxes and questions that emerged from earlier studies. This includes explanations for the characteristic time evolution of D/O events, the different spatial patterns of climate change for D/O and Heinrich events, the recovery of NADW formation after Heinrich events, the fact that cooling pre-dates the iceberg release during Heinrich events and the fact that interglacial climate is much less variable than glacial climate.

Model and background climate

We use the CLIMBER-2 coupled climate model of intermediate complexity[16,17], designed for long-term climate simulations. The model has a coarse spatial resolution, allowing us to resolve only the continental-scale features and different oceanic basins. The atmosphere model is based on the statistical-dynamical approach, and does not resolve synoptic variability; the synoptic fluxes are parameterized as diffusion terms with a turbulent diffusivity computed from atmospheric stability and horizontal temperature gradients. The vertical structures of temperature, specific humidity and meridional atmospheric circulation are parametrized. These parametrizations compute the vertical profiles of temperature, humidity and velocity that are used for calculating the three-dimensional advective, diffusive and radiative fluxes. The latter are computed using a multilevel radiation scheme (16 levels) that accounts for water vapour, ozone, CO_2 and the computed cloud cover (stratiform and cumulus). The ocean model is a multi-basin, zonally averaged model similar to that of ref. 18. This model does not resolve the gyre circulation, so that meridional transports of heat and salt are solely due to the meridional overturning circulation and diffusion, except for the North Atlantic, where freshwater transport due to the subpolar gyre circulation is parametrized (see Methods). The sea-ice model predicts ice thickness and concentration and includes ice advection. In the hierarchy of models, our model is placed between energy balance models and general circulation models (GCMs). On a workstation, the model can be integrated for about 10,000 model years in a day.

A number of sensitivity studies (for example, global warming scenarios[19], and reproducing the climate state without NADW formation found in ref. 20) have shown good agreement with GCM results[15,17]. The model has been used to simulate the climate of the Last Glacial Maximum at 21,000 years before present (21 kyr BP)[15] (for a comparison with other models see ref. 21) and other time slices (Holocene optimum at 6 kyr BP[22], Eemian interglacial at 125 kyr BP[23], and glacial inception at 115 kyr BP). A tran-

sient Holocene experiment[24] (9 kyr BP to the present) has also been performed.

The glacial climate simulation[15] was forced by prescribed orbital changes, and by changes in atmospheric CO_2 concentrations, continental ice, and sea level. A central result was the change in Atlantic Ocean circulation, most importantly a southward shift in the site of Atlantic deep-water formation. The simulations presented here were performed with an improved version of the CLIMBER-2 model; most notably, the latitudinal and vertical resolution of the ocean model was increased to 2.5° and 20 levels, respectively. Land vegetation cover for the glacial climate was computed by the vegetation submodel[25,26] of CLIMBER-2. The new model version reproduces all the important features of our earlier glacial simulation.

Stability of the glacial conveyor

Figure 1 shows stability diagrams of the Atlantic circulation with respect to freshwater flux (the most important control parameter) for both modern and glacial climates. Black curves show the standard advective stability diagram as given in ref. 27, where fresh water was added outside the oceanic convection regions; the red curves were computed by adding fresh water directly to the latitudes of the Nordic Seas. The hysteresis loops are narrower in the latter case because a shut-down or start-up of convection is triggered locally before the basin-scale advective stability limits (bifurcation points) are reached.

The stability diagrams reveal a number of important differences between the modern and glacial climates. As in most other models[20,28], for present-day forcing (Fig. 1a, c) there are two

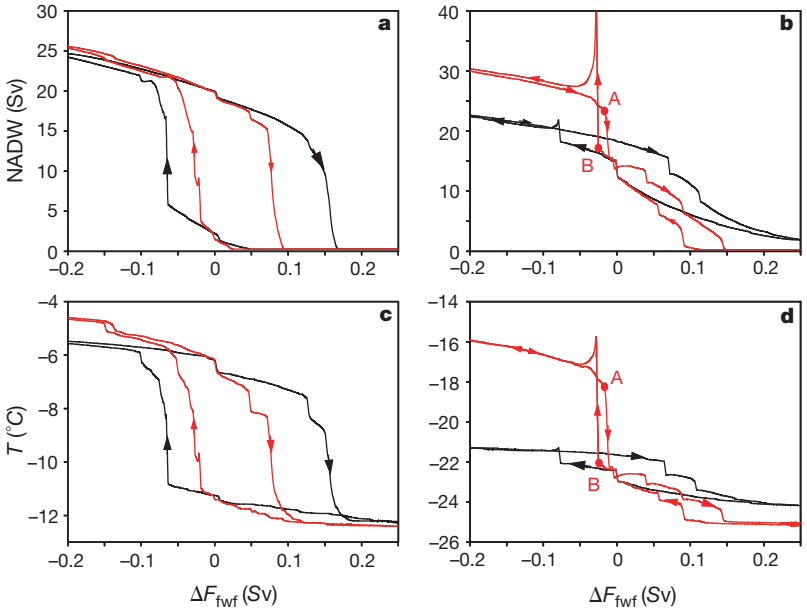

Figure 1 Stability diagrams for the Atlantic thermohaline circulation in the coupled model. The present climate (left panels) differs substantially from the glacial climate (right panels). To calculate the stability diagram the method of ref. 27 was used. The freshwater perturbation ΔF_{fwf} was added in the latitude belt 20–50° N to obtain the black curves, and in the latitude belt 50–70° N to obtain the red curves. Panels **a** and **b** show the ocean circulation response to the freshwater input (in terms of the maximum value of the Atlantic stream function, labelled NADW for North Atlantic Deep Water flow; 1 Sv = 10^6 m^3 s^{-1}), while panels **c** and **d** show the North Atlantic sector air temperature (60–70° N).

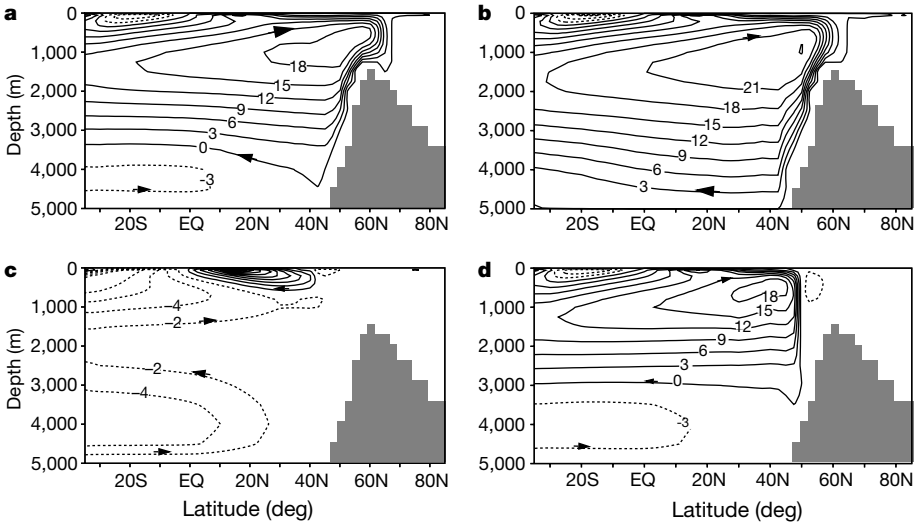

Figure 2 Modes of Atlantic thermohaline circulation in the coupled model. **a**, Holocene 'warm' mode. **b**, Glacial 'warm' (or interstadial) mode. **c**, Holocene 'off' mode. **d**, Glacial 'cold' (or stadial) mode. The diagrams show the stream function (in Sv) for the Atlantic; the model's bottom topography (representing the sill between Atlantic and Nordic seas) is shaded.

fundamentally different climate modes in the CLIMBER-2 model: with and without NADW formation, that is, the 'warm' conveyor belt mode (Fig. 2a) and the 'off' mode (Fig. 2c). The 'width' of the hysteresis loop in freshwater space is proportional to the oceanic heat transport, as it is the buoyancy gain related to releasing this heat to the atmosphere which has to overcome the buoyancy loss resulting from freshwater input in order to trigger convection. The basin-scale stability threshold, that is, the amount of freshwater input that can be sustained before the circulation breaks down, can be computed from a simple conceptual model[28] as

$$F^{\mathrm{crit}} = \frac{\alpha}{4\beta c_p \rho S_0} Q \qquad (1)$$

where α and β are the thermal and haline expansion coefficients, c_p and ρ are the heat capacity and density of sea water, S_0 is a reference salinity and Q is the Atlantic heat transport. For a heat transport of 10^{15} W (roughly the present-day heat-transport maximum in subtropical latitudes, both in our model and in observations) this formula results in a hysteresis width of 0.24 Sv, close to the 0.22 Sv seen in Fig. 1a (black curve).

The stability diagrams for the glacial climate have a rather different shape (Fig. 1b, d). Hysteresis 'width' is similar because the Atlantic heat transport peaks at 1.0×10^{15} W at 20° N in the glacial mode, just as in the modern mode. But when freshwater inflow to the Atlantic is increased the circulation declines gradually, rather than reaching a clear bifurcation point where the circulation breaks down. When the freshwater inflow is decreased again, the hysteresis behaviour is much less pronounced than in the present climate. The reason is that in the modern climate NADW formation is geographically locked into the Nordic Seas—it cannot jump to the south of the sill near Iceland, because temperatures there are too warm. NADW formation must occur near the sea-ice margin, otherwise it is not dense enough to compete with Antarctic Bottom Water (AABW). In the glacial mode, in contrast, it is cold enough for NADW to form south of Iceland (see Fig. 2d) in the open Atlantic. There it is not geographically locked into place, and the conveyor belt is able to respond to surface freshwater input by gradually retreating southwards and becoming shallower. This leads to a smoother, less nonlinear response compared to the modern conveyor belt. A consequence is that for the unperturbed glacial climate there is no 'off' mode and only the 'cold' conveyor belt mode (Fig. 2d) is stable.

Another important difference between glacial and modern climates is seen in the response to freshwater forcing in the latitudes of the Nordic Seas (red curves). For a small negative (that is, evaporative) anomaly the circulation jumps to a 'glacial warm mode' (Fig. 2b) at point B in Fig. 1. This jump is associated with an increase in Greenland temperature of 5 °C (Fig. 1d). The oceanic heat transport across 60° N is 0.12×10^{15} W in this case, and the argument used for the whole Atlantic above can also be applied for the smaller loop of the conveyor belt extending across this latitude into the Nordic Seas in the warm mode: from equation (1) a hysteresis 'width' (distance between points A and B) of about 0.01 Sv should apply (taking into account the smaller value of α for the colder glacial waters), as is indeed found in the model experiment. The proximity of A and B to each other in Fig. 1 is thus explained. The reason why the ocean circulation operates only in two distinctly different modes and transitions between these modes can be triggered by small changes in freshwater flux (that is, the reason for the proximity of A and B to zero in Fig. 1) is the glacial surface freshwater flux, which differs substantially from the present one. Owing to a drastic reduction of precipitation and river runoff to the Arctic the freshwater flux is close to zero here, while in the latitude belt 40–60° N it is much higher than for present-day conditions. The latter is a consequence of a reduction of evaporation, a southward shift of the storm track and a melting of sea ice in this area. This maximum of the freshwater flux serves as a barrier for the penetration of Atlantic water masses to the north. This is why convection in the cold (stadial) mode is locked southward of this 'barrier' and at the same time a relatively small negative freshwater flux applied to the Nordic Seas can start convection there. As a result NADW formation 'jumps' between these locations separated by 1,500 km but cannot be sustained between them.

The different stability properties of the glacial and the modern conveyor belt are thus at least physically plausible. We performed a series of sensitivity experiments to confirm that they are also robust in our model. In these experiments we used a series of different background climates, from full glacial to modern, by varying the prescribed continental ice-sheet size and/or atmospheric CO_2 concentration. We also used a broad range of parameters in the parametrizations of freshwater exchange between the Arctic and the Atlantic (freshwater bypass and sea-ice export, explained in the Methods). These showed that the features shown in Figs 1 and 2 are indeed robust: (1) The glacial climate has a stable 'cold mode' (Fig. 2d) with deep water forming south of the Icelandic sill, and a marginally unstable 'warm mode' (Fig. 2b) which resembles the modern conveyor belt. (2) The conveyor 'off' mode is unstable for glacial conditions.

In addition, the sensitivity study showed that the colder the climate and/or the weaker the export of fresh water from the Nordic Seas, the more points A and B in Fig. 1 move to the left—that is, the more stable the 'cold mode' becomes and the larger the freshwater perturbation required to trigger a transition to the 'warm mode'.

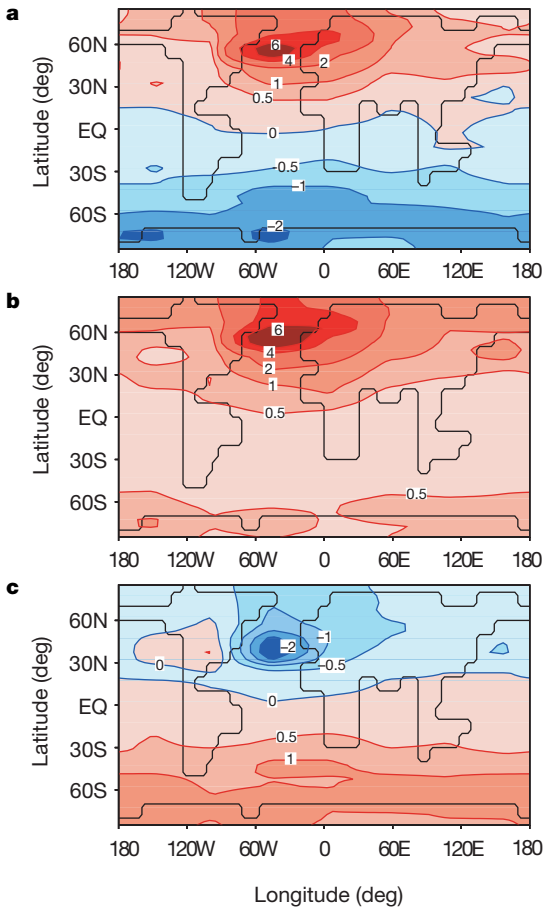

Figure 3 Differences in model-simulated annual mean surface air temperature (°C). **a**, Glacial 'warm' mode (Fig. 2b) minus stadial mode (Fig. 2d) in equilibrium. **b**, Warmest phase of a Dansgaard–Oeschger cycle minus stadial phase, 750 years apart (see Fig. 5d). **c**, Conditions during a Heinrich event minus stadial mode (see Fig. 5d). The full time evolution of surface temperature can be viewed as a movie (see Supplementary Information).

The three qualitatively different circulation modes found in the model coincide with the three circulation modes deduced from palaeoclimate data[29]. The difference in surface temperature between the warm and cold glacial modes is shown in Fig. 3a; it is centred on the northern North Atlantic where it exceeds 6 °C. The Atlantic oceanic heat transport in the glacial warm mode peaks at 1.3×10^{15} W at 20° N compared to 1.0×10^{15} W for the cold mode (Holocene warm mode: 1.0×10^{15} W), but more important for the warming is the fact that the heat transport reaches further north in the warm mode and reduces the area of sea ice in the Northern Hemisphere by one-third.

Dansgaard–Oeschger events

Spectral time-series analysis[30,31] of Greenland ice-core data (Fig. 4) reveals a dominant peak at a periodicity of 1,470 years associated with the D/O events. Our hypothesis is that a weak cycle (of unknown origin) with this period exists in the climate system, and that this cycle could trigger transitions in the Atlantic Ocean circulation. To test this hypothesis, we imposed a periodic variation in the freshwater forcing of the Atlantic in the latitude belt 50–80° N (Fig. 5a) The amplitude of this forcing is very small (about 30 cm yr^{-1} in surface flux or 0.03 Sv in total, compare to Fig. 1); it could, for example, represent changes in river runoff, sea-ice export, shifts in the Atlantic storm track or changes in mass balance of the adjacent ice sheets.

The response to the imposed forcing is shown in Fig. 5. After a period of decreasing freshwater input into the region corresponding to the Nordic Seas, convection is triggered there and a sudden incursion of warm, salty Atlantic water occurs. This represents a flip from the 'cold' to the 'warm' conveyor belt mode (transition B in Fig. 1b). As usual when convection is triggered after a period of stagnation, stored potential energy is released from the water column leading initially to a vigorous flush. Given that the 'warm' mode is not stable under glacial conditions, it gradually decays over the next several hundred years. Finally, a threshold is crossed where convection in the latitudes of the Nordic Seas stops and the system falls back into the stable 'cold' mode. It remains there until the next event is triggered.

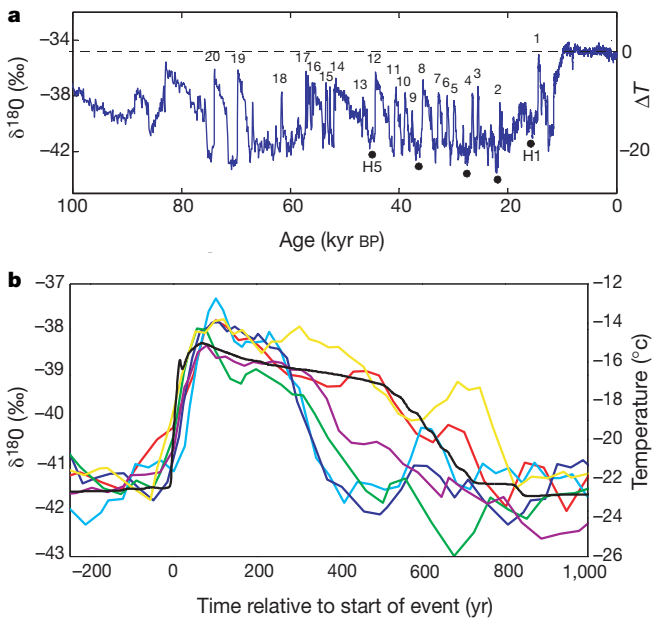

Figure 4 Abrupt climate changes in Greenland ice-core data. **a**, Record of $\delta^{18}O$ from the GRIP core[46], a proxy for atmospheric temperature over Greenland (approximate relative temperature range[47] (in °C) is given on the right). The glacial climate is punctuated by Dansgaard–Oeschger (D/O) warm events (numbered). The timing of Heinrich events H1–H5 is marked by black dots. **b**, Time evolution of recent D/O events taken from **a** (no. 3, light blue; no. 4, dark blue; no. 5, purple; no. 6, green; no. 7, orange; no. 10, red). Many D/O events show the characteristic slow cooling phase after the initial warming, followed by a more abrupt temperature drop. Some events are much longer but still show this general characteristic (for example, nos 8, 12, 19, 20). For comparison, a modelled D/O event is shown in black. For the model we show the North Atlantic sector air temperature 60–70° N (scale on the right), which is a proxy for Greenland temperature in our coarse-resolution model.

This cycle has a characteristic salinity signal (Fig. 5c) in the high latitudes as a result of the salt-water incursions, which far exceeds the direct salinity changes due to the imposed freshwater forcing and which matches the observed salinity variations at this latitude[32].

A characteristic time evolution of Greenland temperatures is associated with the simulated sequence of events (Figs 4b, 5d): an abrupt initial warming, then a gradual cooling trend terminated by a rapid temperature drop back to stadial conditions. Many of the observed D/O events have similar characteristics (Fig. 4b). In Antarctica, temperatures are increasing during the stadial phase and decreasing during the warm event, but the amplitude of the response is small.

It is important that the characteristics of the simulated D/O events do not depend on the imposed forcing cycle. The forcing only acts as a trigger; once an event is set off it follows its own internal dynamics. If the same experiment is performed with different amplitudes of the forcing cycle, then the threshold behaviour becomes clear: for an amplitude of 0.015 Sv no D/O events are triggered and the Greenland temperature remains constant, whereas for a forcing amplitude of 0.045 Sv the events evolve in the same way and with the same amplitude as shown for 0.03 Sv (Fig. 5b–e), except that they are triggered slightly earlier in the cycle.

The surface temperature response (defined as the temperature of the warm phase of a cycle minus the temperature of the cold phase of that cycle) is shown in Fig. 3b. Like the equilibrium difference between the 'warm' and 'cold' conveyor belt modes (Fig. 3a), the region of maximum response is centred on the northern North Atlantic. However, owing to the thermal inertia of the oceans the transient response has the same sign globally, and there is stronger D/O warming in the subtropical Atlantic, in better agreement with palaeoclimatic data from this region. In the Southern Hemisphere the effect of the D/O cycles is weak.

Heinrich events

To simulate Heinrich events a much larger freshwater perturbation was added to the northern North Atlantic (amplitude up to 0.15 Sv, Fig. 5a), which mimics the effect of a major ice-sheet surge[33]. In response to this freshwater release, the conveyor belt shuts down and the system makes a transition to the 'off' mode of Atlantic circulation (Figs 5b, 2c). As the stability diagram (Fig. 1b) shows, this is not a stable circulation mode under glacial conditions, so that the conveyor belt restarts spontaneously after the freshwater influx comes to an end.

What is most interesting is the surface temperature response in Greenland and in Antarctica (Fig. 5d, e). At the start of the Heinrich event the circulation is already in the stadial mode, and Greenland is already cold and beyond the reach of the conveyor belt, so that in Greenland there is hardly any further cooling. This is an important agreement with the Greenland palaeo record (Fig. 4), which shows similar stadial temperatures irrespective of the occurrence of Heinrich events. The strongest cooling caused by the conveyor-belt collapse occurs further south in the subtropical Atlantic[34] (Fig. 3c). This is supported by palaeoceanographic sea surface temperature data from the Mediterranean[35] and the Atlantic off Portugal[36], where Heinrich events register much more strongly than D/O events. The same is true for Antarctica: Heinrich events show the bipolar see-saw with a much stronger Antarctic response, which is due to the dramatic drop in interhemispheric heat transport resulting from the collapse of the conveyor belt[37]. The sequence of

events in Antarctica shows a gradual warming during Greenland stadials and a cooling during Greenland interstadials. These features agree well with the palaeo record[11].

The main difference from previous model studies is that we do not attempt to explain a cooling in Greenland as a consequence of a Heinrich event; instead, we have assumed that the Heinrich event occurs when the climate is already in a cold stadial state, and we show that a Heinrich event in this case leads to no further cooling in Greenland.

Stability of glacial versus modern climate

Previous attempts to model rapid climate changes have started from the present-day Atlantic circulation state, and have focused on modelling cold events as a reduction or collapse of NADW formation triggered by episodic freshwater inflow into the Atlantic[38–41]. This explanation is problematic for glacial conditions, when the climate system stayed for many thousands of years in a cold (stadial) state during periods of accumulation, not melting, of ice sheets. Moreover, improved dating accuracy has made it clear that Heinrich events (associated with large freshwater input into the North Atlantic) occurred after major cooling events in Greenland and could therefore not be their cause.

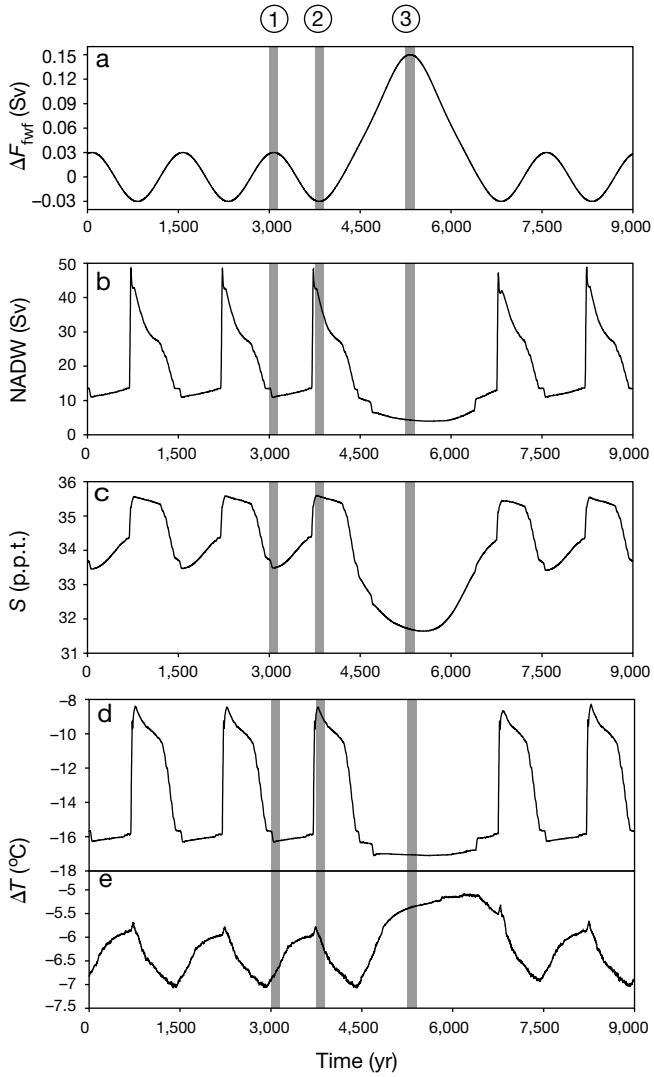

Figure 5 Simulated D/O and Heinrich events. **a**, Forcing, **b**, Atlantic overturning, **c**, Atlantic salinity (S) at 60° N, **d**, air temperature in the northern North Atlantic sector (60–70° N), and **e**, temperature over Antarctica (temperature values are given as the difference from the present-day climate, ΔT). The vertical bars denote the times for which the difference plot is shown in Fig. 3b, c. The time sequence from model year 3,000 to 7,500 of this experiment can be viewed as a movie (see Supplementary Information).

The results of our CLIMBER-2 simulations suggest that the cold stadial periods are the normal mode of operation of the glacial climate system, representing the only stable mode of the glacial Atlantic Ocean circulation: the 'cold' conveyor mode with NADW formation south of Iceland. This realization shifts the focus from modelling 'cold events' to understanding 'warm events'.

Our simulations show that warm events—which are similar to the observed D/O events in time evolution, amplitude and spatial pattern—can be triggered in the model as a temporary flip to the 'warm' conveyor mode with NADW formation in the Nordic Seas. A low-amplitude cycle in freshwater forcing is sufficient to trigger these events. What causes this cycle is not considered here—it could, for example, be ultimately due to solar variability[42]. We merely wish to demonstrate how a weak climate cycle can trigger large-amplitude episodic warm events due to the nonlinear threshold response of the Atlantic Ocean circulation.

Heinrich events, simulated in the model as a large freshwater release during a stadial, lead to a collapse of NADW formation but no major further cooling in Greenland, in agreement with the observed record. Both Heinrich and D/O events are inherently transient as the respective Atlantic circulation modes, the 'off' and the 'warm' modes, are unstable under glacial conditions.

For present-day climate the situation is the reverse, with the 'warm' and the 'off' modes representing the two stable Atlantic circulation states. Our stability analysis thus suggests that a warm climate favours the 'warm' conveyor belt mode (deep-water formation in the Nordic Seas), and a cold climate favours the 'cold' conveyor belt mode (deep-water formation south of Iceland). In the 'cold' mode, transient 'flips' to the 'warm' mode are easily triggered. The exact threshold value depends on the model details, but the crucial fact that it is very small is robust and underpinned by theoretical considerations. We also expect that the real climate will not have one fixed threshold value, but that this varies with the background climate. It is a robust result of our sensitivity study that the glacial 'cold' mode becomes more stable the colder the conditions get, that is, it gets harder to trigger 'flips' to the 'warm' mode. This could explain why the conveyor belt stays predominantly in the 'cold' mode during the coldest parts of the glacial[43], while D/O events occur almost each 1,500-year cycle during more moderate glacial conditions (50–30 kyr BP). As the climate ranges between interglacial (stable warm Atlantic mode) and full glacial (stable cold Atlantic mode) conditions, it passes through a parameter range where it 'flickers' between these two modes.

Once the system is in the 'warm' mode with convection in latitudes north of Iceland, it becomes insensitive to the applied, weak 1,500-year forcing cycle (this experiment was performed but is not detailed here). The freshwater budget of the Nordic Seas is then dominated by the vigorous circulation; anomalies in surface forcing cannot accumulate to create noticeable salinity anomalies as in the stratified 'cold' mode. For this reason, the Holocene climate in our model is stable with respect to the 1,500-year forcing cycle, while the glacial climate is not. We can thus explain the large fluctuations of Greenland temperature during the glacial climate in terms of ocean circulation instability, requiring only a weak trigger but not necessarily any major ice-sheet instability. In the Holocene, the 1,500-year cycle is still present[44] but is not amplified by ocean circulation instability, so that its signature is only weak. □

Methods

Arctic freshwater budget

At present about 0.1 Sv of fresh water (about half of the total Arctic freshwater balance) escapes from the Arctic[45] via the Canadian archipelago and the East Greenland current (in the form of low-salinity surface currents and sea-ice transport) without mixing with the incoming salty Atlantic water. This is an important mechanism which stabilizes convection in the Nordic Seas. This process cannot be explicitly described in a zonally averaged

ocean model, and this leads to an unrealistically low threshold for convective instability of the thermohaline circulation. We therefore developed a parametrization of the freshwater bypass which is included in the new version of the CLIMBER-2 model (in contrast to the version used in ref. 15—we note that the glacial maximum simulation results do not depend on this). The parametrization has two components.

Freshwater bypass by currents

We apply an additional northward mass transport in the upper layers of the North Atlantic between 50° N and 70° N (maximum at 60° N) which mimics the gyre circulation in this region. The same amount of water is returned with a salinity equal to the average salinity between 60° N and 70° N. Thus this parametrization produces a zero net meridional mass transport but a non-zero meridional salinity transport, proportional to the local salinity gradient. The value of the gyre mass transport was tuned to obtain the corresponding observed present-day freshwater transport (0.08 Sv). For glacial conditions, this mass transport was reduced by 50% to take into account the closing of the Canadian archipelago by ice sheets and the partial closure and shallowing of the Denmark Strait. Only the quantitative details, but not the main conclusions, of this work depend on this choice.

Sea-ice export

Our parametrization of ice export is based on the assumption that the export of sea ice from the Nordic seas is proportional to the amount of sea ice in each grid cell and to the meridional wind stress. Exported ice is taken from each grid cell between 60° N and 80° N and is added to the grid cell located 1,000 km further south. Thus the total ice volume is preserved, but a southward sea-ice transport arises which adds to the freshwater transport. For modern climatic conditions this sea-ice export from the Nordic Seas is relatively small (about 0.03 Sv), but it increases during glacial conditions when the Nordic Seas were covered by ice during most of the year.

Received 5 June; accepted 13 November 2000.

1. Heinrich, H. Origin and consequences of cyclic ice rafting in the northeast Atlantic Ocean during the past 130,000 years. *Quat. Res.* **29,** 143–152 (1988).
2. Dansgaard, W. *et al.* A new Greenland deep ice core. *Science* **218,** 1273–1277 (1982).
3. Dansgaard, W. *et al.* Evidence for general instability of past climate from a 250-kyr ice-core record. *Nature* **364,** 218–220 (1993).
4. Clark, P. U., Webb, R. S. & Keigwin, L. D. *Mechanisms of Global Climate Change at Millennial Time Scales* (American Geophysical Union, Washington DC, 1999).
5. Alley, R. B. & Clark, P. U. The deglaciation of the Northern Hemisphere: a global perspective. *Annu. Rev. Earth Planet. Sci.* **27,** 149–182 (1999).
6. Stocker, T. Past and future reorganisations in the climate system. *Quat. Sci. Rev.* **19,** 301–319 (2000).
7. Stocker, T. F. Abrupt climate changes: from the past to the future—a review. *Int. J. Earth Sci.* **88,** 365–374 (1999).
8. Stuiver, M. & Grootes, P. M. GISP2 oxygen isotope ratios. *Quat. Res.* **53,** 277–284 (2000).
9. Alley, R. B., Anandakrishnan, S. & Jung, P. Stochastic resonance in the North Atlantic. *Paleoceanography* (in the press).
10. Sowers, T. & Bender, M. Climate records covering the last deglaciation. *Science* **269,** 210–214 (1995).
11. Blunier, T. *et al.* Asynchrony of Antarctic and Greenland climate climate change during the last glacial period. *Nature* **394,** 739–743 (1998).
12. Stocker, T. F. The seesaw effect. *Science* **282,** 61–62 (1998).
13. Sarnthein, M. *et al.* Changes in east Atlantic deepwater circulation over the last 30,000 years: Eight time slice reconstructions. *Paleoceanography* **9,** 209–267 (1994).
14. Keigwin, L. D., Curry, W. B., Lehman, S. J. & Johnsen, S. The role of the deep ocean in North Atlantic climate change between 70 and 130 kyr ago. *Nature* **371,** 323–326 (1994).
15. Ganopolski, A., Rahmstorf, S., Petoukhov, V. & Claussen, M. Simulation of modern and glacial climates with a coupled global model of intermediate complexity. *Nature* **391,** 350–356 (1998).
16. Petoukhov, V. *et al.* CLIMBER-2: A climate system model of intermediate complexity. Part I: Model description and performance for present climate. *Clim. Dyn.* **16,** 1–17 (2000).
17. Ganopolski, A. *et al.* CLIMBER-2: A climate system model of intermediate complexity. Part II: Model sensitivity. *Clim. Dyn.* (in the press).
18. Stocker, T. F. & Wright, D. G. A zonally averaged ocean model for the thermohaline circulation. Part II: Interocean circulation in the Pacific Atlantic basin system. *J. Phys. Oceanogr.* **21,** 1725–1739 (1991).
19. Rahmstorf, S. & Ganopolski, A. Long-term global warming scenarios computed with an efficient coupled climate model. *Clim. Change* **43,** 353–367 (1999).
20. Manabe, S. & Stouffer, R. J. Two stable equilibria of a coupled ocean-atmosphere model. *J. Clim.* **1,** 841–866 (1988).
21. Kageyama, M. *et al.* The Last Glacial Maximum climate over Europe and western Siberia: a PMIP comparison between models and data. *Clim. Dyn.* **17,** 23–43 (2001).
22. Ganopolski, A., Kubatzki, C., Claussen, M., Brovkin, V. & Petoukhov, V. The role of vegetation-atmosphere-ocean interaction for the climate system during the mid-Holocene. *Science* **280,** 1916–1919 (1998).
23. Kubatzki, C., Montoya, M., Rahmstorf, S., Ganopolski, A. & Claussen, M. Comparison of a coupled global model of intermediate complexity and AOGCM for the last interglacial. *Clim. Dyn.* **16,** 799–814 (2000).
24. Claussen, M. *et al.* Simulation of an abrupt change in Saharan vegetation in the mid-Holocene. *Geophys. Res. Lett.* **26,** 2037–2040 (1999).
25. Brovkin, V., Ganopolski, A. & Svirezhev, Y. A continuous climate-vegetation classification for use in climate-biosphere studies. *Ecol. Model.* **101,** 251–261 (1997).
26. Claussen, M., Brovkin, V., Kubatzki, C., Ganopolski, A. & Petoukhov, V. Modelling global terrestrial vegetation-climate interaction. *Phil. Trans. R. Soc. Lond. B* **353,** 53–63 (1998).
27. Rahmstorf, S. Bifurcations of the Atlantic thermohaline circulation in response to changes in the hydrological cycle. *Nature* **378,** 145–149 (1995).
28. Rahmstorf, S. On the freshwater forcing and transport of the Atlantic thermohaline circulation. *Clim. Dyn.* **12,** 799–811 (1996).
29. Alley, R. B., Clark, P. U., Keigwin, L. D. & Webb, R. S. in *Mechanisms of Global Climate Change at Millennial Time Scales* (eds Clark, P. U., Webb, R. S. & Keigwin, L. D.) 385–394 (American Geophysical Union, Washington DC, 1999).
30. Yiou, P. *et al.* Paleoclimatic variability inferred from the spectral analysis of Greenland and Antarctic ice-core data. *J. Geophys. Res.* **102,** 26441–26454 (1997).
31. Grootes, P. M. & Stuiver, M. Oxygen 18/16 variability in Greenland snow and ice with 10^3- to 10^5-year time resolution. *J. Geophys. Res.* **102,** 26455–26470 (1997).
32. Kreveld, S. V. *et al.* Potential links between surging ice sheets, circulation changes, and the Dansgaard–Oeschger cycles in the Irminger Sea, 60-18 kyr. *Paleoceanography* **15,** 425–442 (2000).
33. Clark, P. U., Alley, R. B. & Pollard, D. Northern hemisphere ice sheet influences on global climate change. *Science* **286,** 1104–1111 (1999).
34. Paillard, D. & Cortijo, E. A simulation of the Atlantic meridional circulation during Heinrich event 4 using reconstructed sea surface temperatures and salinities. *Paleoceanography* **14,** 716–724 (1999).
35. Cacho I. *et al.* Dausgaard–Oeschger and Heinreich event imprints in the Alboran Sea paleotemperatures. *Paleoceanography* **14,** 698–705 (1999).
36. Bard, E., Rostek, F., Turon, J.-L. & Gendreau, S. Hydrological impact of Heinrich events in the subtropical Northeast Atlantic. *Science* **289,** 1321–1324 (2000).
37. Stocker, T. F. & Marchal, O. Abrupt climate change in the computer: is it real? *Proc. Nat. Acad. Sci. USA* **97,** 1362–1365 (2000).
38. Stocker, T. F. & Wright, D. G. Rapid transitions of the ocean's deep circulation induced by changes in surface water fluxes. *Nature* **351,** 729–732 (1991).
39. Manabe, S. & Stouffer, R. Coupled ocean-atmosphere model response to freshwater input: Comparison to Younger Dryas event. *Paleoceanography* **12,** 321–336 (1997).
40. Fanning, A. F. & Weaver, A. J. Temporal-geographical meltwater influences on the North Atlantic conveyor: implications for the Younger Dryas. *Paleoceanography* **12,** 307–320 (1997).
41. Marchal, O., Stocker, T. F. & Joos, F. in *Mechanisms of Global Climate Change at Millennial Time Scales* (eds Clark, P. U., Webb, R. S. & Keigwin, L. D.) 263–284 (American Geophysical Union, Washington DC, 1999).
42. Van Geel, B. *et al.* The role of solar forcing upon climate change. *Quat. Sci. Rev.* **18,** 331–338 (1999).
43. McManus, J. F., Oppo, D. W. & Cullen, J. L. A 0.5-million-year record of millennial-scale climate variability in the North Atlantic. *Science* **283,** 971–975 (1999).
44. Bond, G. *et al.* A pervasive millennial-scale cycle in North Atlantic Holocene and glacial climates. *Science* **278,** 1257–1266 (1997).
45. Aagaard, K. & Carmack, E. C. The role of sea ice and other fresh water in the Arctic circulation. *J. Geophys. Res.* **94,** 14485–14498 (1989).
46. Grootes, P. M., Stuiver, M., White, J. W. C., Johnsen, S. & Jouzel, J. Comparison of oxygen isotope records from the GISP2 and GRIP Greenland ice cores. *Nature* **366,** 552–554 (1993).
47. Dahl-Jensen, D. *et al.* Past temperatures directly from the Greenland Ice Sheet. *Science* **282,** 268–279 (1998).

Supplementary information is available on *Nature*'s World-Wide Web site (http://www.nature.com) or from the London editorial office of *Nature*.

Correspondence and requests for materials should be addressed to A.G. (e-mail: ganopolski@pik-potsdam.de).